J Mol Model (2011) 17:795–803
DOI 10.1007/s00894-010-0762-0

ORIGINAL PAPER

Studying the mechanism that enables paullones to selectively inhibit glycogen synthase kinase 3 rather than cyclin-dependent kinase 5 by molecular dynamics simulations and free-energy calculations

Quan Chen · Wei Cui · Yuanhua Cheng · Fushi Zhang · Mingjuan Ji

Received: 15 January 2010 / Accepted: 17 May 2010 / Published online: 19 June 2010

Abstract Glycogen synthase kinase 3 (GSK-3) is an attractive target for the treatment of diabetes, and paullones have been reported to be effective inhibitors of GSK-3. However, it is still a challenging task to improve selectivity among protein kinases, especially cyclin-dependent kinases (CDKs). Here we investigated the mechanism that enables paullones to selectively inhibit GSK-3 rather than cyclin-dependent kinase 5 (CDK5) using sequence alignment, molecular dynamics simulations, free-energy calculations and free-energy decomposition analysis. The results indicate that the interaction between paullones and Val135 of GSK-3 is obviously stronger than that between paullones and Cys83 of CDK5, suggesting that paullones could be utilized as potent selective inhibitors. Meanwhile, we observed that the decrease in the interaction between paullones and the Asp86 of CDK5 favors their selectivity towards GSK-3 rather than CDK5, as demonstrated using 1-azakenpaullone as an example. Although substitution at position 9 and replacement at position 2 may influence the activity of GSK-3, they only have a minor effect on the selectivity. We expect that the information obtained here could prove useful for developing specific paullone inhibitors of GSK-3.

Electronic supplementary material The online version of this article (doi:10.1007/s00894-010-0762-0) contains supplementary material, which is available to authorized users.

Q. Chen · W. Cui · M. Ji (✉)
College of Chemistry and Chemical Engineering,
Graduate University of Chinese Academy of Sciences,
Beijing 100049, People's Republic of China
e-mail: jmj@gucas.ac.cn

Y. Cheng · F. Zhang
Key Laboratory of Organic Optoelectronics and Molecular Engineering of Ministry of Education, Department of Chemistry,
Tsinghua University,
Beijing 100084, People's Republic of China

Keywords Glycogen synthase kinase 3 · Cyclin-dependent kinase 5 · Paullones · Selectivity · Molecular dynamics simulation · Binding free energy

Introduction

The prevalence and rising incidence of diabetes has become one of the most serious threats to global public health [1]. There are 220 million people worldwide who have diabetes, and this number is likely to reach 300 million by 2025 [2]. Therefore, new targets and novel therapeutic drugs against diabetes are urgently required.

As reported, glycogen synthase kinase 3 (GSK-3) is an important factor in the regulation of glucose metabolism. The inactivation of glycogen synthase by phosphorylation through GSK-3 results in decreased glycogen synthesis [3]. Thus, GSK-3 has become an attractive drug target for diabetes, and various groups around the world have attempted to design novel GSK-3 inhibitors over the past decade [4–8]. One such GSK-3 inhibitor is paullone, which was reported in 2000 [4].

Since GSK-3 is closely related to the cyclin-dependent kinases (CDKs) [8], it is not surprising that most GSK-3 inhibitors have been found to act on both GSK-3 and CDKs such as alsterpaullone [4]. In 2004, Kunick reported that 1-azakenpaullone displays 200-fold greater selectivity for GSK-3 than for cyclin-dependent kinase 5 (CDK5) [9]. Based on that work, a series of inhibitors were synthesized [10]. However, it is still a challenge to improve selectivity for GSK-3 rather than CDKs.

In this study, the mechanism that enables the selectivity of paullones towards GSK-3 rather than CDK5 was investigated by molecular dynamics (MD) simulations, molecular mechanics/Poisson–Boltzmann surface area (MM/PBSA) free-energy calculations [11–19], and molecular mechanics/

generalized Born surface area (MM/GBSA) free-energy decomposition analysis [20–23]. We expect that this work could provide useful information for the development of more promising specific paullone inhibitors of GSK-3. The chemical structures of the inhibitors studied in this work are shown in Fig. 1 [4, 9, 10].

Materials and methods

Starting structure

The crystallographic structure of GSK-3 complexed with alsterpaullone (PDB entry: 1Q3W) was obtained from the RCSB Protein Data Bank (PDB) [24]. Since some of the residues in 1Q3W were missing, it was necessary to complete the chain of this complex. Therefore, 1O9U, the X-ray diffraction structure of GSK-3 complexed with a different inhibitor was selected as the initial structure of GSK-3, as this structure has a complete chain [25]. In order to construct the complex structures of 1O9U and the inhibitors, the models 1Q3W and 1O9U were structurally aligned by homology using the biopolymer module of SYBYL7.1 [26], and the alsterpaullone ligand in 1Q3W was extracted and merged into 1O9U. The structure of 1O9U complexed with alsterpaullone was taken as the starting point for the following calculations. The complexes of 1-azakenpaullone/GSK-3 and 2-azakenpaullone/GSK-3 were derived from the alsterpaullone/GSK-3 complex.

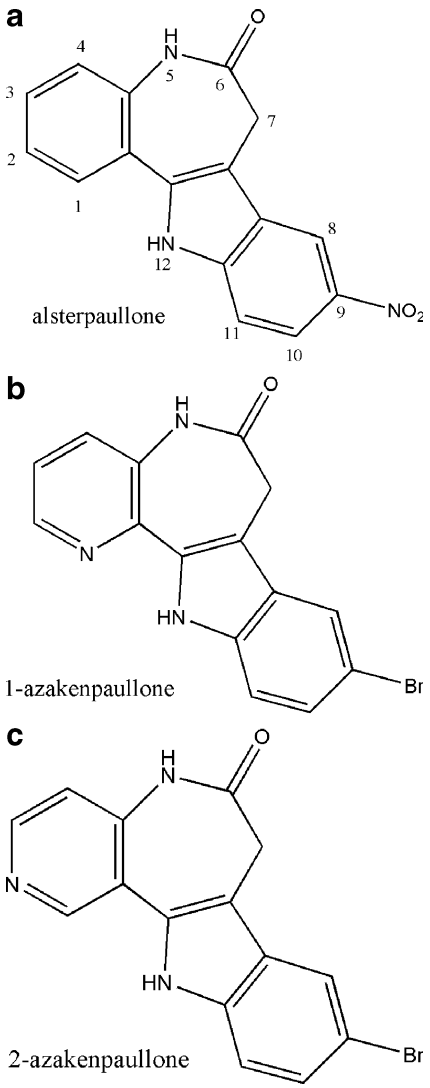

Fig. 1 Structures of the inhibitors studied in this work: alsterpaullone, 1-azakenpaullone and 2-azakenpaullone [4, 9, 10]

The crystallographic structure of CDK5 (PDB entry: 1UNL) was also obtained from the RCSB Protein Data Bank [27]. This complex has two chains that are the same, so only chain A was selected as the initial structure of CDK5. The complex of each inhibitor with CDK5 was constructed as follows: first, the CDK5 and GSK-3 complexes were structurally aligned; then the ligand in GSK-3 was extracted and merged into CDK5. The root mean square deviation (RMSD) of the alpha carbons between the two proteins was only 2.3830 Å, which indicates their similarity and confirms that the above method is a feasible one for constructing complexes of CDK5.

All of the above work was performed using the molecular modeling package SYBYL7.1 [26]. The missing atoms of GSK-3 and CDK5 were added using the *leap* program in AMBER9.0 [28]. The AMBER03 force field was used to establish the potentials of the proteins [29], while the general AMBER force field (*gaff*) [30] was used to establish the potentials of the inhibitors. Each complex was immersed in TIP3P water [31] in a truncated octahedron box that extended 12 Å away from any solute atom. Cl^- ions were then added to neutralize the system using *leap* in AMBER9.0.

To obtain the minimized geometries for electrostatic potential calculations, the inhibitors (with Gasteiger–Hückel charges) were first minimized using the conjugate gradient method to a gradient of 0.001 kcal $mol^{-1}Å^{-1}$ in SYBYL7.1. Further geometric optimization was then performed with Gaussian 03 [32] using the Hartree–Fock/6-31G* level of theory. Subsequently, the atomic charges of the inhibitors were derived by fitting the electrostatic potentials calculated by Gaussian 03 using the restrained electrostatic potential (RESP) technique [33]. Partial atomic charges and *gaff* forcefield parameters for the inhibitors were generated by the *antechamber* program in AMBER9.0 [30].

Sequence alignment

In order to compare differences in the binding sites, sequence alignment was performed on GSK-3 and CDK5,

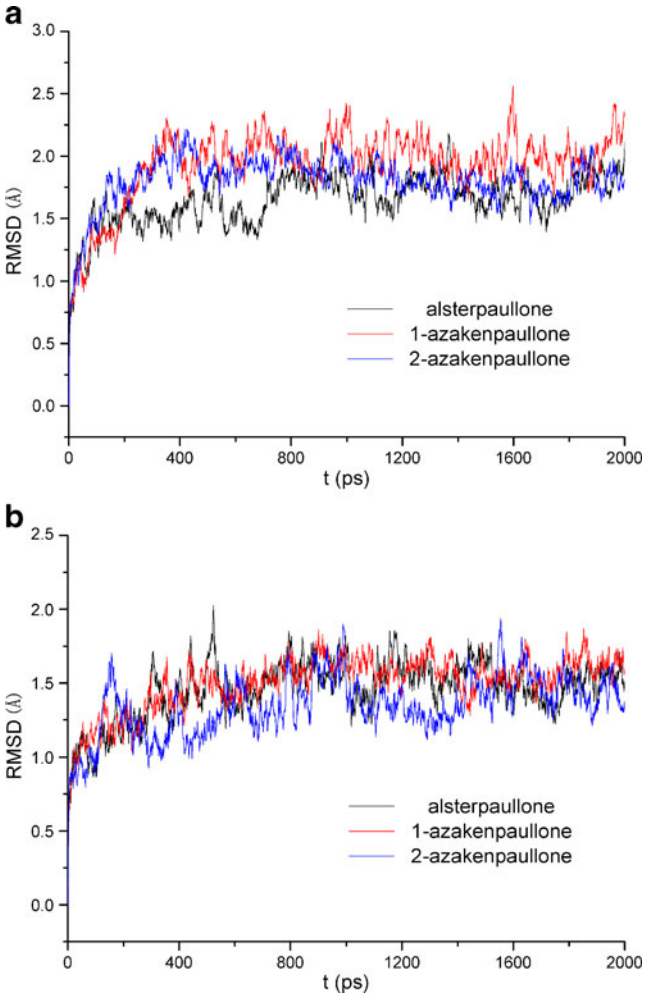

Fig. 2 RMSDs of the backbone atoms of **a** GSK-3 and **b** CDK5 complexed with inhibitors

which will provide useful information for the analysis of binding free energy and for improving the inhibitors. The alignment was performed using EMBOSS online (provided by the European Bioinformatics Institute, EBI). *Needle* was selected to find the optimum alignment of the two sequences, and the parameters used for the gap open penalty, gap extend penalty and the matrix were 10, 0.5 and Blosum62, respectively [34, 35].

Molecular dynamics simulations

Prior to the MD simulations, energy optimization was conducted using the *sander* program in AMBER9.0 in three steps. First, the water molecules were optimized via steepest descent minimization for 2000 cycles, followed by a conjugate gradient minimization for 2000 cycles. Then, all of the backbone atoms were restrained, and the side chains, inhibitor and solvent were optimized using 5000 steps of steepest descent and 10000 steps of conjugate gradient minimization. Finally, the whole system was optimized using 5000 steps of steepest descent and 5000 conjugate gradient minimization without any restraint.

After optimization, the system was gradually heated from 0 K to 310 K over 60 ps. Then, 2 ns MD simulations were performed with a 2 fs time step and the SHAKE algorithm [36] under a constant temperature of 310 K using the weak-coupling algorithm [37]. Particle-mesh Ewald (PME) was employed to treat the long-range electrostatic interactions [38, 39]. The coordinates were saved every 1 ps, and the conformations generated from these simulations were used for binding free-energy calculations and decomposition analysis.

Calculation of the binding free energies

Using the trajectories generated by MD simulations, the binding free energies (ΔG_{bind}) of the inhibitors as well as the individual energy components were calculated using an

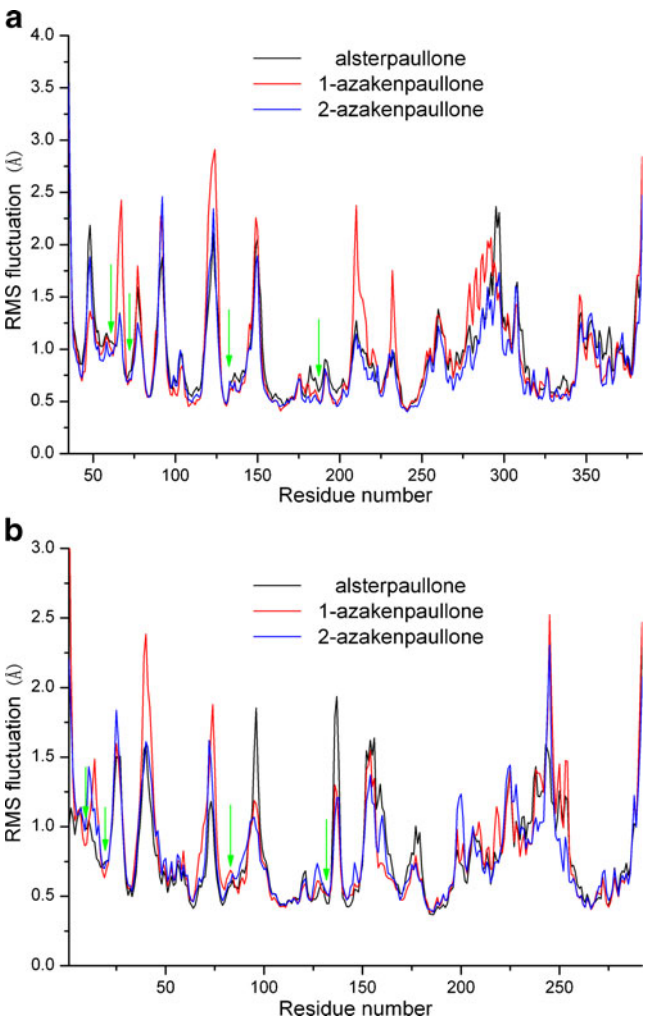

Fig. 3 RMSFs of the backbone atoms of **a** GSK-3 and **b** CDK5 complexed with inhibitors

Table 1 Binding free energies and energy components of inhibitors (kcal mol^{-1})

Ligand-protein complex	ΔE_{vdw}	ΔE_{ele}	ΔG_{PB}	$\Delta E_{ele}+\Delta G_{PB}$	ΔG_{SA}	$-T\Delta S$	ΔG_{pred}	IC_{50}(nM) [4, 9, 10]
Alsterpaullone/GSK-3	−37.38±3.18	−14.72±4.16	24.52±3.11	9.80	−4.93±0.17	−13.14	−45.65	0.004
Alsterpaullone/CDK5	−39.37±2.51	−33.27±5.73	47.69±4.38	14.42	−4.88±0.12	−10.58	−40.42	0.040
1-Azakenpaullone/GSK-3	−37.76±2.64	−10.02±3.48	21.23±3.19	11.21	−4.87±0.12	−14.78	−46.20	0.018
1-Azakenpaullone/CDK5	−36.11±2.77	−24.06±5.44	39.35±3.30	15.29	−4.91±0.13	−10.37	−36.10	4.200
2-Azakenpaullone/GSK-3	−38.33±2.67	−19.12±3.33	30.55±2.65	11.43	−4.88±0.10	−13.59	−45.37	0.052
2-Azakenpaullone/CDK5	−35.99±2.63	−37.30±7.36	47.22±4.57	9.92	−4.83±0.11	−11.67	−42.57	0.180

MM/PBSA procedure according to the following equation [18, 19]:

$$\begin{aligned}\Delta G_{bind} &= G_{complex} - G_{protein} - G_{ligand} \\ &= \Delta E_{MM} + \Delta G_{PB} + \Delta G_{SA} - T\Delta S\end{aligned} \quad (1)$$

where ΔE_{MM} is the molecular mechanics interaction energy between the protein and inhibitor; ΔG_{PB} and ΔG_{SA} are the polar and nonpolar free energies of solvation, respectively; and $T\Delta S$ is the entropic contribution of the inhibitor at temperature T.

Here, the polar solvation energy was calculated by solving the Poisson–Boltzmann (PB) equations. The nonpolar solvation contribution was calculated as: G_{SA}= 0.0072×SASA [40]. The binding free energy of the inhibitor was calculated by averaging the 160 snapshots extracted from the MD trajectory from 0.4 to 2.0 ns at 10 ps intervals. The conformational entropy upon ligand binding was calculated using normal-mode analysis by the *nmode* program in AMBER9.0 [28]. Each snapshot was fully minimized for 100,000 steps in the presence of a distance-dependent dielectric of $4r_{ij}$ (r_{ij} is the distance between two atoms) until the root mean square of the elements of the gradient vector was less than 1.0×10^{-3}kcal mol^{-1} $Å^{-1}$. Due to the high computational demand of this approach, only 20 snapshots that were evenly extracted from the MD trajectory from 0.4 to 2.0 ns were used to calculate the entropic contribution.

Decomposition analysis of the binding free energies

An MM/GBSA decomposition process was employed to calculate the interaction between the inhibitor and each residue using the *mm_pbsa* program in AMBER9.0 [22]. The interaction of each inhibitor–residue pair includes three energy terms: a van der Waals contribution (ΔE_{vdw}), an electrostatic contribution (ΔE_{ele}), and a solvation contribution ($\Delta G_{solvation}$). The solvation free energy $\Delta G_{solvation}$ is the sum of the polar (ΔG_{GB}) and the nonpolar (ΔG_{SA}) parts. The ΔG_{GB} term was computed using the generalized Born (GB) model, and the parameters for GB were developed by Onufriev et al. [9]. The nonpolar contribution (ΔG_{SA}) was determined based on the solvent-accessible surface area (SASA), as determined with the ICOSA method [41]. In this method, the SASA per atom was estimated with a recursive algorithm, and at every recursion step each triangular face of the polyhedron is divided into four pieces of equal size, allowing a better approximation of a sphere to be obtained. All of the above energy components were calculated using 160 snapshots, as generated above.

Results and discussion

MD simulations were performed on six inhibitor/protein complexes. The root mean square displacements (RMSDs) of the backbone atoms of the GSK-3 and CDK5 complexes

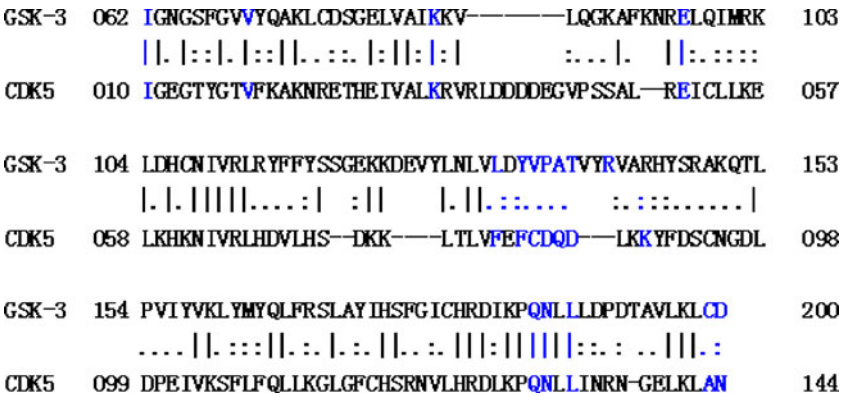

Fig. 4 Sequence alignment of GSK-3 and CDK5

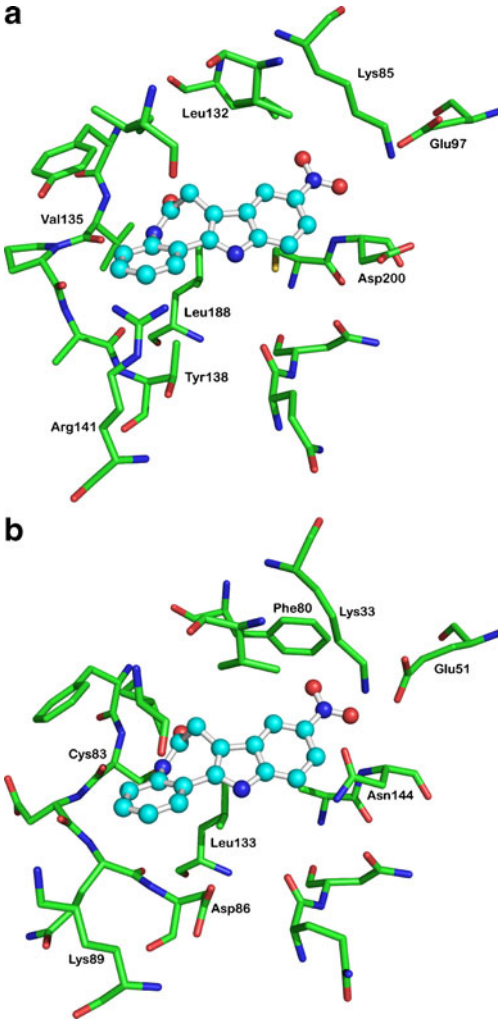

Fig. 5 Comparison of the residues that interact with the inhibitor in **a** GSK-3 and **b** CDK5

were calculated and are plotted in Fig. 2. From this figure, it can be seen that the RMSDs of the GSK-3 and CDK5 complexes achieved equilibrium at 0.4 ns, and fluctuated at around 2.0 Å and 1.5 Å, respectively. Although 2 ns is a very short simulation, the trajectories are stable enough for the following binding free-energy calculations and free-energy decomposition analysis. In addition, other characters such as the RMSDs of the inhibitors and the distances between key atoms in GSK-3 and CDK5 were also calculated (shown in the "Electronic supplementary material"), which further confirmed the stability of the simulations.

More detailed analysis of the root mean square fluctuations (RMSFs) versus the residue numbers of the six complexes is illustrated in Fig. 3. Overall, structures with the same proteins share similar RMSF distributions and similar trends in dynamic features. Meanwhile, the residues of both GSK-3 and CDK5 around the binding sites indicated by arrows in Fig. 3 show rigid behavior. Thus, inhibitions should be due to similar interactions on the whole.

Binding free energy

In the MM/PBSA calculations, the affinity of a ligand for binding to a protein can be estimated by the snapshots from the trajectory of the complex. The binding free energies and the energy components of inhibitors are shown in Table 1. An excellent correlation (r=0.858) is observed between the experimental results ($\ln IC_{50}$) and the predicted values.

According to the energy components of the binding free energies, ΔE_{vdw} contributes most to the binding free energies and ΔG_{SA} contributes slightly favorably. The net electrostatic contribution (the sum of ΔE_{ele} and ΔG_{PB}) opposes the binding.

Selectivity mechanism for inhibitors

As inhibitors of GSK-3, paullones show better activity towards GSK-3 rather than CDK5 on the whole. In the current work, we discuss their selectivity towards GSK-3 rather than CDK5 from two aspects. First, we investigate

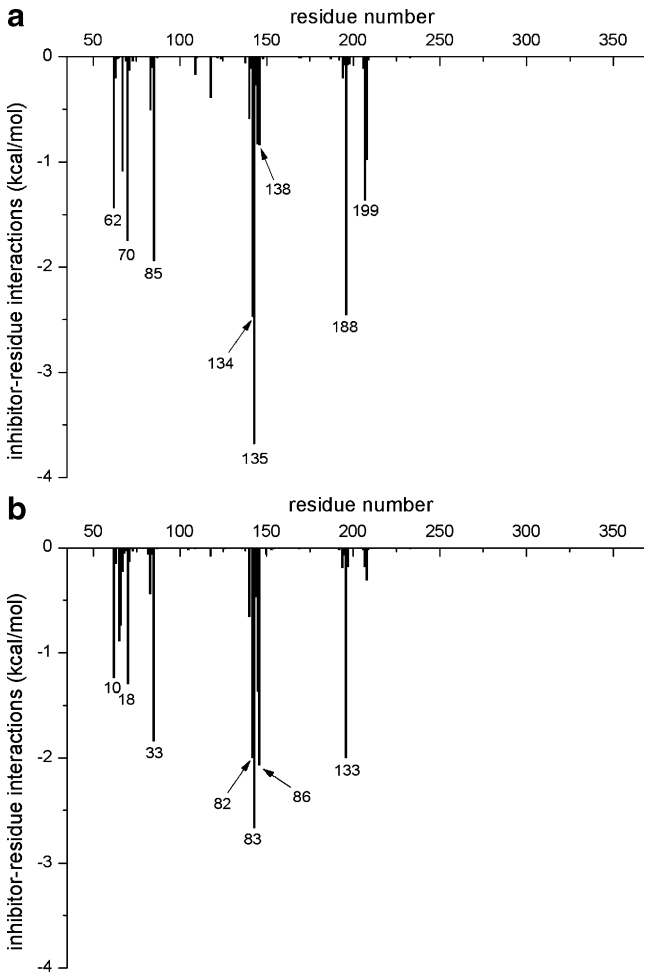

Fig. 6 Inhibitor–residue interaction spectra of alsterpaullone with **a** GSK-3 and **b** CDK5

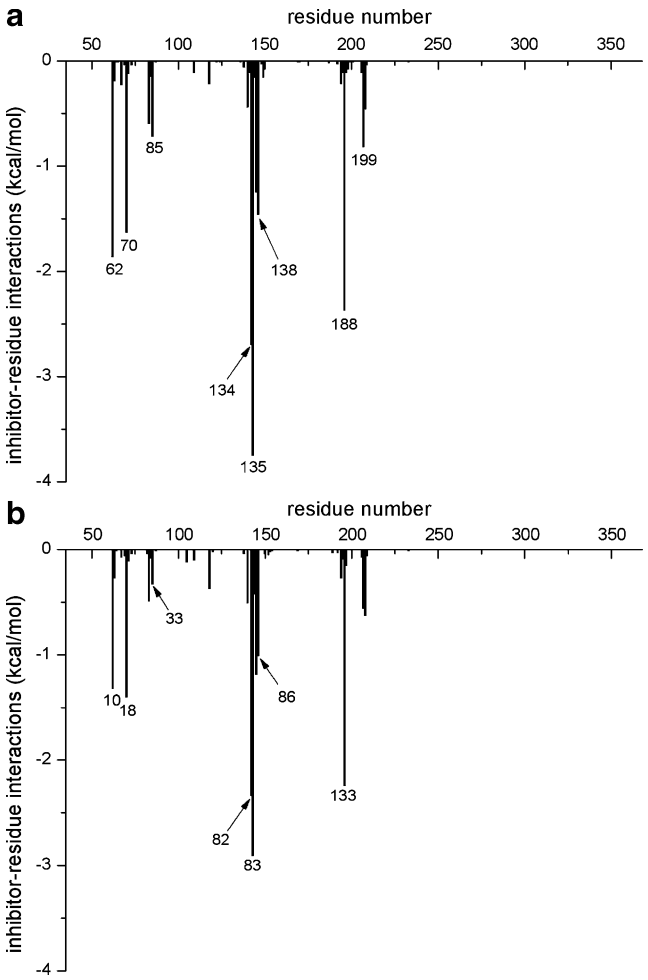

Fig. 7 Inhibitor–residue interaction spectra of 1-azakenpaullone with **a** GSK-3 and **b** CDK5

why paullones have an inherent selectivity towards GSK-3 rather than CDK5. Second, we study the selectivity mechanism of 1-azakenpaullone. In addition, considering that the selectivity of an inhibitor is determined by the dissimilarity between the proteins, especially the differences in residues around the binding sites, it is necessary to compare the protein sequences of GSK-3 and CDK5. In this work we used EMBOSS to compare the sequences of the proteins. The sequence identity of the two proteins is 28.8% and their similarity is 45.4%. The result of sequence alignment for GSK-3 and CDK5 is shown in Fig. 4, in which the residues that can interact with the inhibitor are highlighted in blue. A comparison of the residues in GSK-3 and CDK5 that interact with the inhibitor is shown in Fig. 5. From this figure, it can be seen that the inhibitor undergoes similar interactions with the two proteins. Meanwhile, it is worth mentioning that although Arg141 of GSK-3 corresponds to a gap, there is a similar position (Lys89) in CDK5, so Arg141 of GSK-3 shows a similar interaction to Lys89 of CDK5.

Based on the above work, free-energy decomposition analysis was employed to discern the detailed interactions between inhibitors and residues, which will provide more quantitative information. The results of the decomposition analysis of inhibitors and residues are shown in Figs. 6, 7 and 8. Moreover, in order to compare the corresponding homologous residue interactions between GSK-3 and CDK5 directly, we added some gaps between the residue numbers in Figs. 6, 7, 8 and 9 based on the gap information provided by sequence alignment. However, the labels are the actual residue series of the proteins.

From Figs. 6a, 7a and 8a, it can be seen that the interactions between the inhibitors and GSK-3 are mainly determined by the following residues: Ile62, Val70, Tyr134, Val135, Ala137, Thr138, Leu188 and Cys199. Figures 5, 6 and 7 indicate that the interaction spectra of GSK-3 and CDK5 are quite similar. Residues such as Ile10, Val18, Phe82, Cys83, Gln85, Asp86, Leu133 and Ala143 of CDK5 also undergo strong interactions with inhibitors. However, interactions with GSK-3 are stronger than those

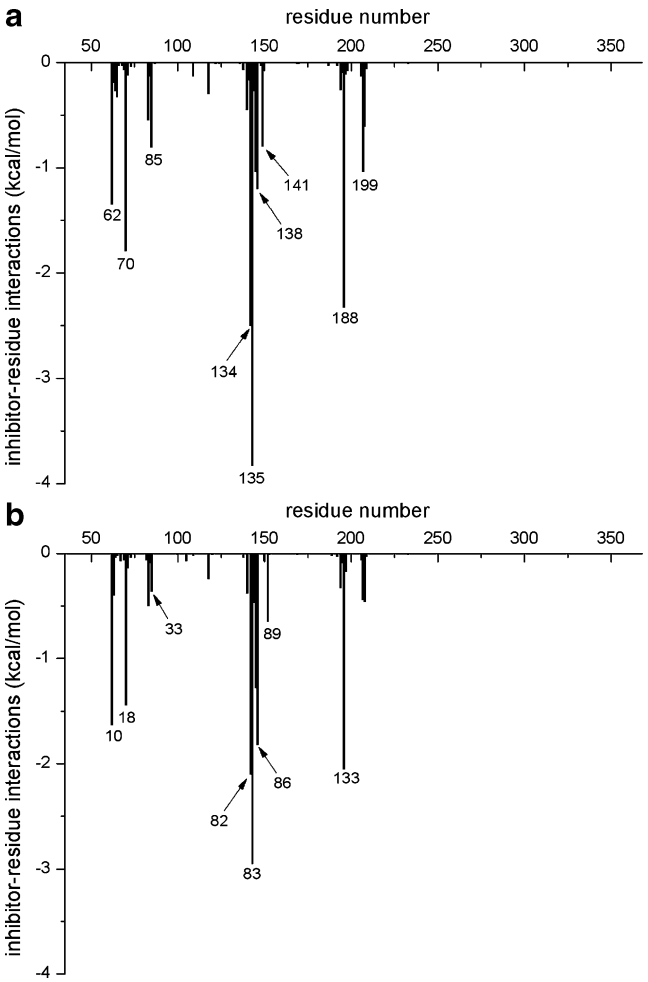

Fig. 8 Inhibitor–residue interaction spectra of 2-azakenpaullone with **a** GSK-3 and **b** CDK5

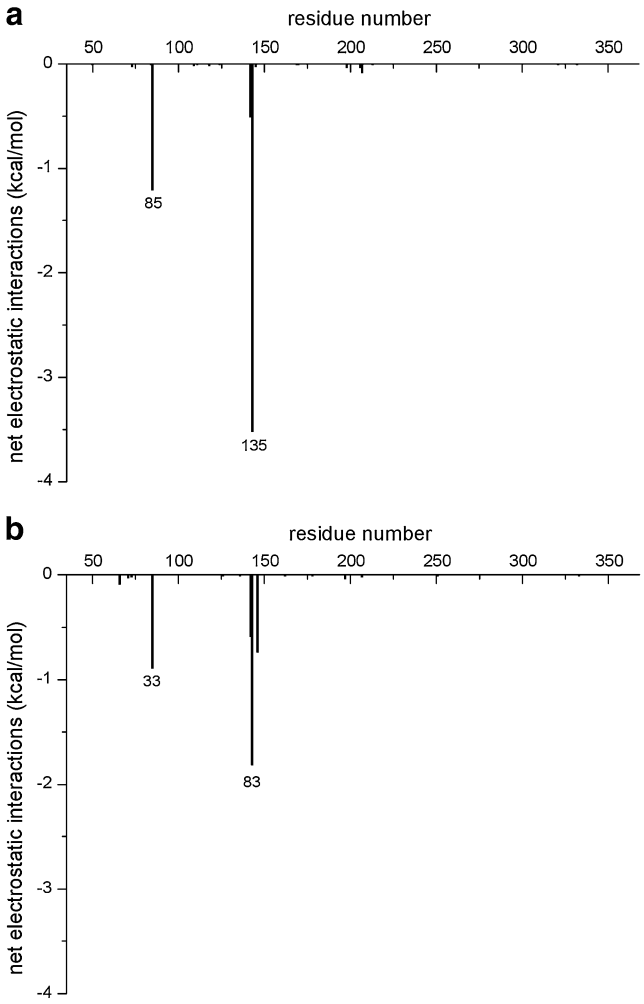

Fig. 9 Comparison of the net electrostatic interactions of alsterpaullone with **a** GSK-3 and **b** CDK5

with CDK5 on the whole, which are consistent with the experimental result that paullones show stronger activities towards GSK-3 rather than CDK5.

By comparing the energy contributions in GSK-3 and CDK5, it was found that all of the ΔE_{VDW} values are similar (data not shown) but that the net electrostatic contributions (sum of ΔE_{ele} and ΔG_{PB}) of GSK-3 are obviously stronger than those of CDK5. Here we take alsterpaullone as an example. As shown in Fig. 9, the net electrostatic contributions of alsterpaullone with Val135 of GSK-3 and Cys83 of CDK5 are −3.52 and −1.82 kcal mol^{-1}, respectively, which are the key factors that cause paullones to exhibit stronger biological activities towards GSK-3 rather than CDK5. However, as suggested by Fig. 5, the inhibitors could interact with the backbone of Val135 in GSK-3 and that of Cys83 in CDK5. Therefore, it is not a wise approach to improve the selectivity by modifying the inhibitor groups that interact with these residues. Hence, it is necessary to find other factors that may influence the selectivity.

Comparing Fig. 5 with Figs. 6 and 7, it is clear that the interactions of alsterpaullone with Lys85 of GSK-3 (−1.94 kcal mol^{-1}) and with Lys33 of CDK5 (−1.84 kcal mol^{-1}) are different from those of 1-azakenpaullone (−0.72 and −0.33 kcal mol^{-1}) and 2-azakenpaullone (−0.81 and −0.36 kcal mol^{-1}). This could be because the nitro group of alsterpaullone can form stronger electrostatic interactions with Lys85 and Lys33. When C9 is substituted by bromine, the interaction clearly decreases. However, whether C9 is substituted by another nitro group or a bromine, the interactions with GSK-3 and CDK5 are similar. Consequently, the substitution of C9 by different groups may have a significant effect on the activity of GSK-3, but it does not have a great effect on the selectivity towards GSK-3 rather than CDK5. By analyzing the residues around C9, it is easy to elucidate this phenomenon. Both Lys85 and Glu97 of GSK-3 around C9 are identical to those of CDK5.

As reported by Kunick, when C1 is substituted by nitrogen, the selectivity towards GSK-3 rather than CDK5 is clearly increased. They inferred that the charge distribution only disturbs the binding of CDKs, not the binding of GSK-3 [9]. In this work we compared the structures after the MD simulations. The distance between the OD2 atom of Asp86 and N12 (~1.91 Å) is shorter than that between the CG2 atom of Thr138 and N12 (~4.50 Å). The N12 of paullones can thus form a hydrogen bond with the Asp86 of CDK5. Meanwhile, free-energy decomposition analysis indicates that position 1 has a great influence on the interaction between N12 and Asp86 of CDK5. As shown in Figs. 6b and 7b, the interactions of Asp86 with alsterpaullone and 1-azakenpaullone are −2.07 and −1.01 kcal mol^{-1}, respectively. In order to confirm this result, the visible percentages of hydrogen bonds during MD simulations were calculated and are shown in Table 2. From Table 2, it can be found that the visible percentage of hydrogen bonds of alsterpaullone with Asp86 (64.00%) is distinctly larger than that of 1-azakenpaullone (39.25%), which is consistent with the results of the decomposition analysis. However, a structural change at position 1 has little effect because N12

Table 2 Visible percentages of hydrogen bonds during MD simulations of CDK5

Inhibitor	Donor	Acceptor	Occupied (%)	Distance (Å)	Angle (°)
Alsterpaullone	:86@O3	:inhi@H-:inhi@N12	64.00	2.84	17.62
1-Azakenpaullone	:86@O3	:inhi@H-:inhi@N12	39.25	2.86	17.25
2-Azakenpaullone	:86@O3	:inhi@H-:inhi@N12	58.69	2.85	14.69

is far from Thr138 of GSK-3 (the corresponding residue of CDK5 is Asp86). It can thus be further concluded that N1 influences the hydrogen bond between the inhibitor and the Asp86 of CDK5 and enhances the selectivity of the inhibitor.

Moreover, as shown in Fig. 5, position 2 of the paullones is close to a basic residue in GSK-3 or CDK5 (Arg141 or Lys89, respectively). Thus, in contrast to 1-azakenpaullone, 2-azakenpaullone can form electrostatic interactions with Arg141 in GSK-3 or Lys89 in CDK5, but as shown in Fig. 8, the interactions (0.80 and 0.65 kcal mol^{-1}) are similar. Therefore, such interactions barely contribute to the selectivity towards GSK-3 rather than CDK5. In addition, although replacing C2 with N2 also decreases the interaction with Asp86, upon comparing Figs. 7b and 8b, we find that the interaction of 2-azakenpaullone with Asp86 (−1.82 kcal mol^{-1}) is stronger than that of 1-azakenpaullone (−1.01 kcal mol^{-1}) in CDK5. Therefore, replacing C2 with nitrogen has less of an effect on the selectivity than replacing C1 with nitrogen.

Conclusions

GSK-3 has emerged as an attractive target for the treatment of diabetes, and paullones have been reported to be effective inhibitors of GSK-3. However, it is still a challenging task to improve selectivity among protein kinases, especially CDKs. In this study, six complexes of three paullone inhibitors were studied. MD simulations and the MM/PBSA technique were employed to calculate the binding free energy. The results obtained are consistent with experimental values. Subsequent studies, such as sequence alignment and free-energy decomposition analysis, demonstrate that different substitutions at C9 may affect the activity of GSK-3, but barely affect the selectivity towards GSK-3 rather than CDK5. Though the difference in the interactions between Val135 of GSK-3 and Cys83 of CDK5 does contribute to the selectivity, this effect is limited. The most effective way of improving the selectivity is to change the interaction with Asp86 in CDK5, as was demonstrated for 1-azakenpaullone.

Acknowledgments The project was supported by the National Science and Technology Major Special Project of China (No. 2009ZX09501-011).

We thank Prof. Xiaojie Xu at the Department of Chemistry of Peking University for providing access to computer software such as AMBER.

References

1. Zimmet P, Alberti K, Shaw J (2001) Global and societal implications of the diabetes epidemic. Nature 414(6865):782–787
2. King H, Aubert RE, Herman WH (1998) Global burden of diabetes, 1995–2025. Prevalence, numerical estimates, and projections. Diab Care 21(9):1414–1431
3. Welsh GI, Proud CG (1993) Glycogen-synthase kinase-3 is rapidly inactivated in response to insulin and phosphorylates eukaryotic initiation-factor elf-2b. Biochem J 294:625–629
4. Leost M, Schultz C, Link A, Wu YZ, Biernat J, Mandelkow EM et al (2000) Paullones are potent inhibitors of glycogen synthase kinase-3 beta and cyclin-dependent kinase 5/p25. Eur J Biochem 267(19):5983–5994
5. Martinez A, Alonso M, Castro A, Perez C, Moreno FJ (2002) First non-ATP competitive glycogen synthase kinase 3 beta (GSK-3 beta) inhibitors: thiadiazolidinones (TDZD) as potential drugs for the treatment of Alzheimer's disease. J Med Chem 45(6):1292–1299
6. Coghlan MP, Culbert AA, Cross DAE, Corcoran SL, Yates JW, Pearce NJ et al (2000) Selective small molecule inhibitors of glycogen synthase kinase-3 modulate glycogen metabolism and gene transcription. Chem Biol 7(10):793–803
7. Leclerc S, Garnier M, Hoessel R, Marko D, Bibb JA, Snyder GL et al (2001) Indirubins inhibit glycogen synthase kinase-3 beta and CDK5/P25, two protein kinases involved in abnormal tau phosphorylation in Alzheimer's disease—a property common to most cycline-dependent kinase inhibitors? J Biol Chem 276(1):251–260
8. Frame S, Cohen P (2001) GSK3 takes centre stage more than 20 years after its discovery. Biochem J 359:1–16
9. Kunick C, Lauenroth K, Leost M, Meijer L, Lemcke T (2004) 1-Azakenpaullone is a selective inhibitor of glycogen synthase kinase-3 beta. Bioorg Med Chem Lett 14(2):413–416
10. Stukenbrock H, Mussmann R, Geese M, Ferandin Y, Lozach O, Lemcke T et al (2008) 9-Cyano-1-azapaullone (cazpaullone), a glycogen synthase kinase-3 (GSK-3) inhibitor activating pancreatic beta cell protection and replication. J Med Chem 51(7):2196–2207
11. Huo SH, Wang JM, Cieplak P, Kollman PA, Kuntz ID (2002) Molecular dynamics and free energy analyses of cathepsin D-inhibitor interactions: insight into structure-based ligand design. J Med Chem 45(7):1412–1419
12. Kuhn B, Kollman PA (2000) Binding of a diverse set of ligands to avidin and streptavidin: an accurate quantitative prediction of their relative affinities by a combination of molecular mechanics and continuum solvent models. J Med Chem 43(20):3786–3791
13. Weis A, Katebzadeh K, Soderhjelm P, Nilsson I, Ryde U (2006) Ligand affinities predicted with the MM/PBSA method: dependence on the simulation method and the force field. J Med Chem 49 (22):6596–6606
14. Wang JM, Morin P, Wang W, Kollman PA (2001) Use of MM-PBSA in reproducing the binding free energies to HIV-1 RT of TIBO derivatives and predicting the binding mode to HIV-1 RT of efavirenz by docking and MM-PBSA. J Am Chem Soc 123(22):5221–5230
15. Hou TJ, Chen K, McLaughlin WA, Lu BZ, Wang W (2006) Computational analysis and prediction of the binding motif and protein interacting partners of the Abl SH3 domain. PLoS Comput Biol 2(1):46–55
16. Hou TJ, Guo SL, Xu XJ (2002) Predictions of binding of a diverse set of ligands to gelatinase-A by a combination of molecular dynamics and continuum solvent models. J Phys Chem B 106(21):5527–5535
17. Hou TJ, Yu R (2007) Molecular dynamics and free energy studies on the wild-type and double mutant HIV-1 protease complexed with amprenavir and two amprenavir-related inhibitors: mechanism for binding and drug resistance. J Med Chem 50(6):1177–1188
18. Wang JM, Hou TJ, Xu XJ (2006) Recent advances in free energy calculations with a combination of molecular mechanics and continuum models. Curr Comput-Aided Drug Des 2(3):287–306
19. Kollman PA, Massova I, Reyes C, Kuhn B, Huo SH, Chong L et al (2000) Calculating structures and free energies of complex molecules: combining molecular mechanics and continuum models. Acc Chem Res 33(12):889–897

20. Hou TJ, McLaughlin W, Lu B, Chen K, Wang W (2006) Prediction of binding affinities between the human amphiphysin-1 SH3 domain and its peptide ligands using homology modeling, molecular dynamics and molecular field analysis. J Proteome Res 5(1):32–43
21. Hou TJ, Zhang W, Case DA, Wang W (2008) Characterization of domain-peptide interaction interface: a case study on the amphiphysin-1 SH3 domain. J Mol Biol 376(4):1201–1214
22. Gohlke H, Case DA (2004) Converging free energy estimates: MM-PB(GB)SA studies on the protein–protein complex Ras-Raf. J Comput Chem 25(2):238–250
23. Hou TJ, McLaughlin WA, Wang W (2008) Evaluating the potency of HIV-1 protease drugs to combat resistance. Proteins 71(3):1163–1174
24. Bertrand JA, Thieffine S, Vulpetti A, Cristiani C, Valsasina B, Knapp S et al (2003) Structural characterization of the GSK-3 beta active site using selective and non-selective ATP-mimetic inhibitors. J Mol Biol 333(2):393–407
25. Dajani R, Fraser E, Roe SM, Yeo M, Good VM, Thompson V et al (2003) Structural basis for recruitment of glycogen synthase kinase 3 beta to the axin–APC scaffold complex. EMBO J 22(3):494–501
26. Vanopdenbosch N, Cramer R, Glarrusso FF (1985) Sybyl, the integrated molecular modeling system. J Mol Graph 3(3):110–111
27. Mapelli M, Massimiliano L, Crovace C, Seeliger MA, Tsai LH, Meijer L et al (2005) Mechanism of CDK5/p25 binding by CDK inhibitors. J Med Chem 48(3):671–679
28. Case DA, Cheatham TE, Darden T, Gohlke H, Luo R, Merz KM et al (2005) The Amber biomolecular simulation programs. J Comput Chem 26(16):1668–1688
29. Duan Y, Wu C, Chowdhury S, Lee MC, Xiong GM, Zhang W et al (2003) A point-charge force field for molecular mechanics simulations of proteins based on condensed-phase quantum mechanical calculations. J Comput Chem 24(16):1999–2012
30. Wang JM, Wolf RM, Caldwell JW, Kollman PA, Case DA (2004) Development and testing of a general amber force field. J Comput Chem 25(9):1157–1174
31. Jorgensen WL, Chandrasekhar J, Madura JD, Impey RW, Klein ML (1983) Comparison of simple potential functions for simulating liquid water. J Chem Phys 79(2):926–935
32. Frisch MJ, Trucks GW, Schlegel HB, Scuseria GE, Robb MA, Cheeseman JR et al (2004) Gaussian 03. Gaussian Inc., Wallingford
33. Bayly CI, Cieplak P, Cornell WD, Kollman PA (1993) A well-behaved electrostatic potential based method using charge restraints for deriving atomic charges—the resp model. J Phys Chem 97(40):10269–10280
34. Needlema SB, Wunsch CD (1970) A general method applicable to search for similarities in amino acid sequence of 2 proteins. J Mol Biol 48(3):443–453
35. Kruskal JB (1983) An overview of sequence comparison—time warps, string edits, and macromolecules. Siam Rev 25(2):201–237
36. Ryckaert JP, Ciccotti G, Berendsen HJC (1977) Numerical-integration of cartesian equations of motion of a system with constraints—molecular-dynamics of N-alkanes. J Comput Phys 23(3):327–341
37. Berendsen HJC, Postma JPM, Vangunsteren WF, Dinola A, Haak JR (1984) Molecular-dynamics with coupling to an external bath. J Chem Phys 81(8):3684–3690
38. Darden T, York D, Pedersen L (1993) Particle mesh Ewald—an N. log(N) method for Ewald sums in large systems. J Chem Phys 98 (12):10089–10092
39. Essmann U, Pereral L, Berkowitz ML, Darden T, Lee H, Pedersen LG (1995) A smooth particle mesh Ewald method. J Chem Phys 103(19):8577–8593
40. Weiser J, Shenkin PS, Still WC (1999) Approximate atomic surfaces from linear combinations of pairwise overlaps (LCPO). J Comput Chem 20(2):217–230
41. Gohlke H, Kiel C, Case DA (2003) Insights into protein–protein binding by binding free energy calculation and free energy decomposition for the Ras–Raf and Ras–RaIGDS complexes. J Mol Biol 330(4):891–913